第57回流体力学講演会/
第43回航空宇宙数値シミュレーション技術シンポジウム
2025年7月2日～4日
タワーホール船堀（東京）

JSASS-2025-2039

1E02 極超音速流可視化のためのグロー放電陽光柱の発光強度の電子平均自由行程依存性

○カオ・ヴァン・ギア，井藤 創，溝口 誠（防衛大学校）

Dependence of emission intensity of glow discharge used for hypersonic flow visualization on electron mean free paths

Nghia Cao Van, Hajime Itoh, Makoto Mizoguchi (National Defense Academy)

Key Words: Hypersonic Flow, Flow Visualization, Positive Column, Mean Free Path

Abstract

To develop a quantitative method for measuring hypersonic flows using glow plasma, this study tries to find parameters that characterize the emission characteristics and systematically examines it. A positive column was generated in stationary air whose pressure was adjusted to match the electron mean free path expected when the column interacts with a hypersonic flow. The emission intensity of the nitrogen second positive band within this column was measured using an ultraviolet camera. It was revealed that the intensity depends not only on the electron mean free path but also on the current density. By formulating the dependence, the potential for quantitative density measurement of hypersonic flows using the glow discharge method was demonstrated.

1. Introduction

Visualizations and quantitative measurements are essential to elucidate the aerodynamic characteristics and the flow phenomena of the flows around hypersonic vehicles. Various methods have been proposed and used in hypersonic flows according to the purposes, environmental circumstances, and characteristics of each method. LIF [1], CARS [2], REMPI [3], and e-beam [4] are used to observe flow fields at molecular level. However, because of low signal intensities, these methods often require complex and expensive apparatus, long measurement times, and numerous trials. On the other hand, the glow discharge method, which our laboratory has focused on, has a high signal intensity and requires a relatively simple measurement system. Furthermore, the discharge method allows for three-dimensional visualization of flow fields [5].

Electric discharges have been widely used over 60 years, primarily as a visualization method [5–10]. In addition, there are also examples of using glow discharge for quantitative measurements. Itoh measured velocity distributions in a hypersonic boundary layer by the glow discharge tracer method [11]. Kimmel et al. used emission spectroscopy of plasma discharge to obtain spatially resolved rotational temperatures within the boundary layer of a flat plate model in a Mach 5.1 flow [12]. Nishio and Itoh tried to explain qualitatively the experiment using the electric discharge to visualize the shock wave [13]. They used the electron impact excitation function to represent the dependence of plasma emission intensity on the energy of electrons colliding with gas atoms or molecules. Assuming a constant electric field (which is determined by dividing the applied voltage between electrodes by the gap distance) in the plasma, they presented the relationship among the electric field, emission intensity, and gas density. However, in glow discharge plasma, the presence of an anode fall and a cathode fall regions prevents the electric field in the positive column from being determined using the above method. Furthermore, the electron impact cross-section in the excitation function used by Nishio and Itoh [13] is only valid for kinetic energies of 13 eV and above, which is too high for typical conditions in glow discharge plasma. A basic theory suitable for glow discharge plasmas must be developed.

In previous research [14], Itoh and Mizoguchi utilized an electric discharge method to visualize hypersonic airflow over a forward-facing step model. They iden-

tified the discharge type as glow discharge and established a simple relationship between the overall emission intensity of the second positive bands and the number density of nitrogen molecules. Their results indicated that the electric field appeared to be uniform along the positive column when interacting with shock waves in hypersonic flow. This condition is particularly significant as it suggests that the electric field increases linearly with the gas number density in complex flow fields. Understanding this phenomenon provides deeper insights not only into the glow discharge measurement methodology but also into the physical characteristics of electric currents penetrating through shock waves. The positive column theory of glow discharges in tubes filled with uniform gases is well established, while the characteristics of positive columns generated in open environments without tubes and interacting with airflow have not been studied extensively.

To develop a quantitative method for measuring hypersonic flows using glow plasma, this study systematically examines the emission characteristic and tries to find parameters that influence it. When glow discharge interacts with hypersonic flow, the electron drift velocity substantially exceeds the flow velocity, allowing us to treat gas particles as effectively stationary relative to electrons. Consequently, we can assume that a positive column in stationary air with the same mean free path as one in hypersonic flow exhibits identical characteristics. To simulate mean free paths comparable to those in the hypersonic flow, we conducted experiments in stationary air at pressures ranging from 390 Pa to 2500 Pa.

2. Relationship between positive column emission intensity, pressure, and other parameters

In previous work, Itoh and Mizoguchi established a relationship among the emission intensity of the second positive band of nitrogen, electric field, and gas number density [14]. Here, we briefly explain the hypothesis they used and extend it further. The emission intensity is given by:

$$I'_{2+} \propto k_1 n_e N \tag{1}$$

where I'_{2+} represents the overall emission intensity of the second positive bands, k_1 is the rate coefficient, n_e is the electron number density, and N is the gas number density. The electron number density can be calculated as:

$$n_e = \frac{I_{\mathrm{gap}}}{e v_e A} \tag{2}$$

where I_{gap} is the electric current between the electrodes, e is the elementary electron charge, v_e is the electron drift velocity, and A is the cross-sectional area of the positive column. From the references [15,16], we have the following relationships:

$$k_1 \propto \left(\frac{E}{N}\right)^{6.7} \tag{3}$$

$$v_e \propto \left(\frac{E}{N}\right)^{0.7} \tag{4}$$

Combining Eqs. (1), (2), (3), and (4), we obtain:

$$I'_{2+} \propto \left(\frac{E}{N}\right)^{6} I_{\mathrm{gap}} A^{-1} N \tag{5}$$

Eq. (5) holds only when collisional quenching is absent and requires correction. Here, we consider the Stern–Volmer relationship:

$$\frac{I'_{2+}}{I_{2+}} = 1 + k_q \tau N \tag{6}$$

where I_{2+} is the emission intensity with collisional quenching accounted for, k_q is the overall quenching coefficient, τ is the emission lifetime of the second positive bands of nitrogen molecules. After accounting for the quenching effect, Eq. (5) becomes:

$$I_{2+}(1 + k_q \tau N) \propto \left(\frac{E}{N}\right)^{6} I_{\mathrm{gap}} R^{-2} N \tag{7}$$

where R is the radius of the positive column. To visualize the positive column, we used an ultraviolet camera to capture images. The brightness B at any y station displayed in the image represents the integrated emission intensity along the line of sight. Thus,

$$B \propto I_{2+} R \tag{8}$$

Substituting this into Eq. (7), we obtain:

$$B(1 + k_q \tau N) \propto \left(\frac{E}{N}\right)^{6} I_{\mathrm{gap}} R^{-1} N \tag{9}$$

Eq. (9) demonstrates that the brightness of the image visualizing the positive column depends on the electric field, gas number density, electrode gap current, and radius of the positive column.

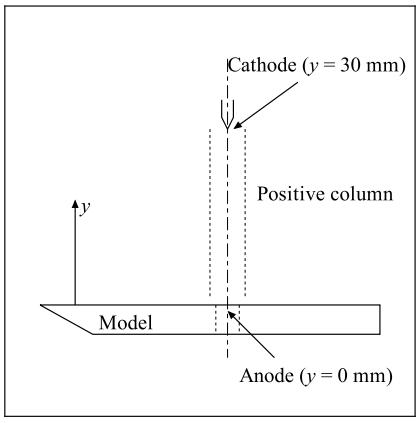

Fig. 1 Model setup

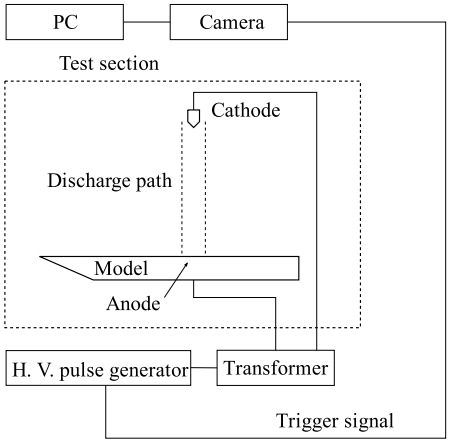

Fig. 2 Experimental setup

3. Experimental setup

3.1. Test section

In this study, the low-pressure environment is provided within a hypersonic tunnel test section, which is a cylindrical chamber with an inner diameter of 1.2 m and a length of 1.6 m. Observation windows, 300 mm in diameter, are installed on both sides of the chamber, allowing visualization using techniques such as Schlieren photography and glow discharge imaging. The test section is connected to a cylindrical vacuum chamber with an inner diameter of 1.2 m and a length of 3.5 m. A vacuum pump is used to depressurize both the test section and the vacuum chamber to approximately 0.1 Pa.

3.2. Test model and arrangement of electrodes

The discharge column is generated between a cathode positioned above the flat plate model and an anode flush with the model surface as shown in Fig. 1. The model was constructed from Bakelite, chosen for its machinability and electrical insulation properties. A hole with a diameter of 6 mm was drilled through the model, allowing a cylindrical copper anode of the same diameter to be inserted such that its surface remained flush with the model surface. The anode was then connected to the transformer's anode via a conductive wire. A tungsten cathode, shaped as a 3 mm diameter rod, was placed 30 mm away from the model surface, with its axis perpendicular to the surface and pointing directly at the anode. The cathode tip was conically shaped with a semi-apex angle of 30°. Except for the tip, the rod was wrapped in Kapton tape to electrically insulate it from the plasma. Before conducting the experiments, all electrode surfaces were cleaned of any debris.

3.3. Glow discharge method

The schematic of the experimental setup is shown in Fig. 2. The ultraviolet camera is set to capture the positive column when the discharge is generated. A detailed description of the circuit has been presented in a previous paper [17].

3.4. UV Camera

In this experiment, we employed an ultraviolet camera (ARTRAY ARTCAM-407UV-WOM) to quantify the emission intensity of the positive column. Since the second positive band exhibits the strongest emission intensity in the positive column, we selected a UV camera with high sensitivity in the corresponding wavelength range. The spectral response characteristic of the UV camera is illustrated in Fig. 3, which demonstrates optimal sensitivity in the region where the nitrogen second positive band emissions are concentrated (primarily 300-400 nm). The detailed specifications and sensi-

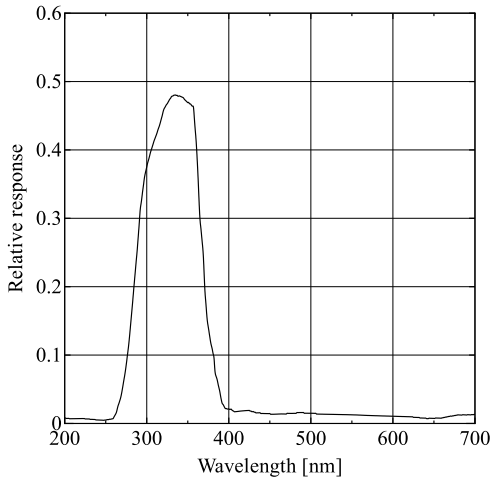

Fig. 3 Spectral response characteristic of the UV camera adopting UV transmitting, visible absorbing filter, reproduced from reference [18)]

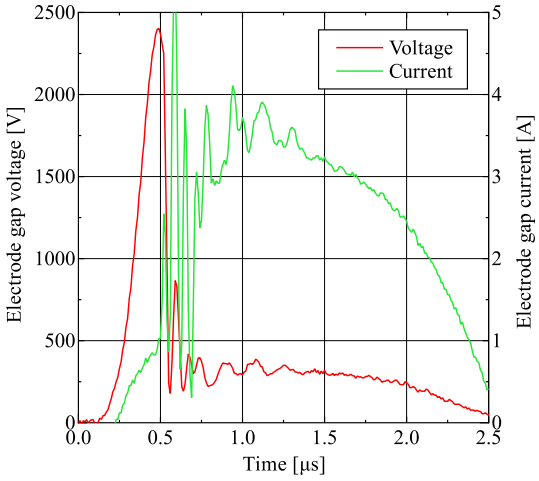

Fig. 4 Current-voltage characteristic of glow discharge in stationary air at $p = 800$ Pa

Table1: Specifications of the UV camera

Sensor Type	CCD Monochrome Image Sensor
Shutter Type	Global Shutter
Shutter Speed	1/58824–1/12.5 s
Resolution	6.5 pixel/mm

tivity characteristics of the camera and lens system are summarized in Table 1.

3.5. Current-voltage measurements

For measuring the anode potential, a high-voltage probe (Tektronix P6015A, input impedance 100 MΩ, input capacitance 3 pF, maximum input voltage 20 kV, rise time 4.67 ns) was employed. For cathode potential measurements, a 10:1 probe (HITACHI AT-10CP, input impedance 10 MΩ, input capacitance 14 pF, maximum input voltage 600 V, rise time 3.5 ns) was utilized.

Current measurements were performed using a current probe (Tektronix P6021A, rise time 3.5 ns, power module Tektronix AM5030).

4. Results

4.1. Glow discharge current-voltage characteristics

A high voltage was applied to induce dielectric breakdown between the electrodes. An example of the current-voltage characteristic of glow discharge in stationary air at 800 Pa is shown in Fig. 4. Immediately after breakdown ($t = 0.5$ μs), a peak voltage of approximately 2.4 kV is applied between the electrodes. This voltage rapidly decreases to approximately 300 V at $t = 0.7$ μs. After minor fluctuations, the voltage stabilizes at approximately 300 V at $t = 1.0$ μs and subsequently decreases gradually to 230 V at $t = 2.0$ μs, before decreasing monotonically to 50 V at $t = 2.5$ μs. The current characteristics exhibit strong fluctuations during the immediate post-breakdown period due to stochastic electron collisions with gas particles. These fluctuations stabilize at approximately $t = 1.0$ μs, with the current decreasing gradually from 3.6 A to 2.4 A at $t = 2.0$ μs, before finally decreasing to 0.4 A at $t = 2.5$ μs. Based on the relative stability of both voltage and current during the interval $1.0\ \mu\text{s} \leq t \leq 2.0\ \mu\text{s}$, we define this period as the self-sustaining discharge phase. The characteristic voltage and current values for this phase are evaluated by temporal averaging over this duration. The electrode gap voltage and current measurements at different pressures are presented in Fig. 5.

In Fig. 5, we observe that the electrode gap voltage increases with pressure, supporting the hypothesis that the electric field increases with gas number density. For pressures other than 390 Pa, the electric current de-

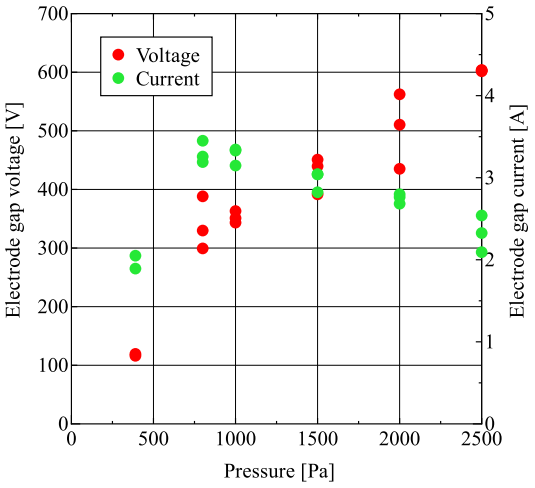

Fig. 5 Electrode gap voltage and current measured at various pressures

creases as pressure increases, which is consistent with findings reported by Baryshnikov [19]. The anomalous behavior at 390 Pa is caused by an abnormally high cathode potential (approximately 130 V), which is unexpected since the cathode is grounded. This deviation may be attributed to the stochastic nature of electron-molecule collisions in glow plasma, which can occasionally produce measurements that deviate from the general trend. During the experiments, we observed that at 390 Pa, the discharge current exhibits significant fluctuations across multiple measurements. When the cathode potential is maintained at a nominally low value (below 30 V), the current is approximately 3.5 A at 390 Pa and follows the expected trend observed in this study. However, to ensure a comprehensive investigation of the relationship between emission intensity and glow discharge characteristics, we utilize the measured current values despite their stochastic nature.

4.2. Emission intensity analysis

The images captured by the UV camera were analyzed to quantify the emission intensity and determine the radius of the positive column. An example of the positive column visualization is shown in Fig. 6, with brightness and contrast adjusted to improve visibility. The transverse brightness distribution at $y = 15$ mm (the

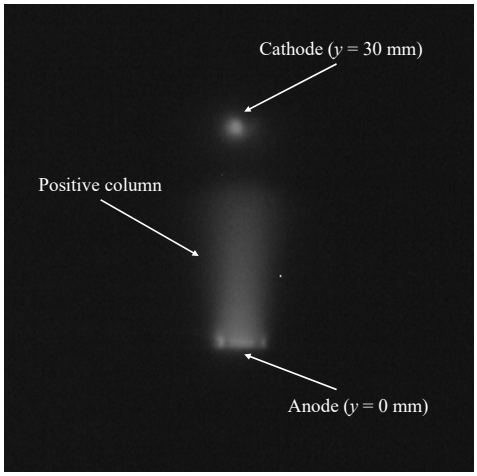

Fig. 6 Visualization of a positive column at $p = 2000$ Pa. Brightness and contrast have been adjusted to improve visibility

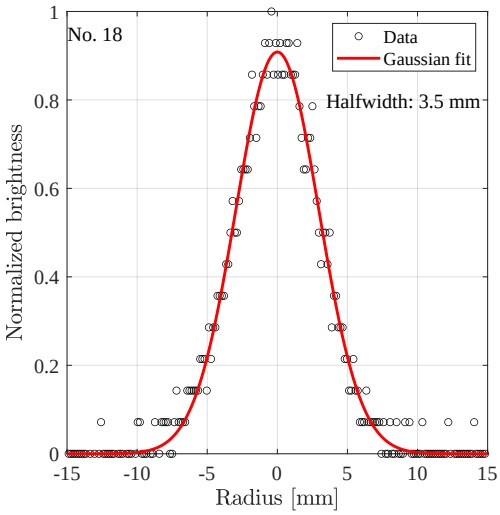

Fig. 7 Example of Gaussian fit for the transverse brightness distribution at $y = 15$ mm of the positive column at $p = 2500$ Pa

center of the electrode gap) of the positive column was used to estimate the current region dimension. An example of these distributions is presented in Fig. 7. In this figure, the brightness is normalized by the central brightness value, which serves as the representative intensity measure for the positive column in this study. The distributions were fitted using a Gaussian function, and the half-width of this distribution, multiplied by the coefficient $\sqrt{3}$, was considered equivalent to the radius of the positive column.

The relationship between ambient pressure and the radius of the positive column is illustrated in Fig. 8.

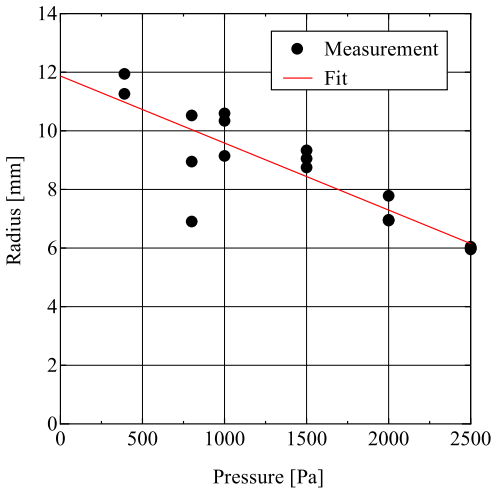

Fig. 8 Relationship between ambient pressure p and the measured radius of the positive column

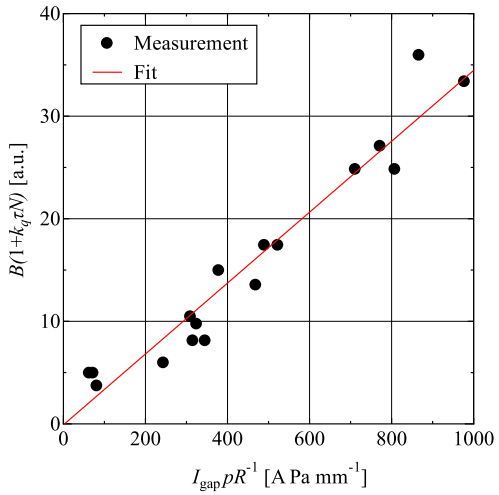

Fig. 9 Relationship between $I_{\mathrm{gap}}R^{-1}p$ and $B(1+k_q\tau N)$

From Fig. 8, it can be observed that as the pressure increases, the radius of the positive column decreases. This inverse relationship was previously documented in research by Baryshnikov et al. [19].

From Eq. (9), if our assumption that the reduced electric field E/N remains constant is valid, then the products $I_{\mathrm{gap}}R^{-1}N$ and $B(1+k_q\tau N)$ should exhibit a proportional relationship. In this study, since the background gas temperature remains constant, Eq. (9) can be rewritten as:

$$B(1+k_q\tau N) \propto I_{\mathrm{gap}}R^{-1}p \tag{10}$$

Fig. 9 demonstrates the relationship between the product $I_{\mathrm{gap}}R^{-1}p$ and the product $B(1+k_q\tau N)$. The figure shows a linear proportional relationship, confirming the assumption that E/N remains approximately constant as pressure increases. Eq. (10) can be rewritten as:

$$I_{2+}(1+k_q\tau N) \propto Jp \tag{11}$$

where J is the current density. From this observation, we can conclude that the emission intensity depends primarily on the ambient pressure and the current density.

4.3. Estimation of the reduced electric field in the positive column

Fig. 10 presents typical reduced electric field values in discharge tubes as reported by Raizer et al. [20]. The

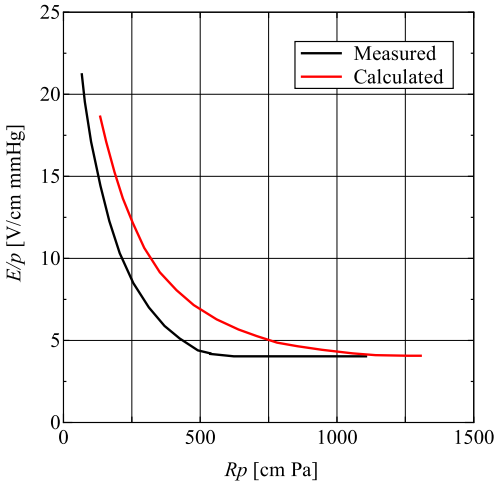

Fig. 10 Empirical values of the reduced electric field in a positive column in plasma tube

red line represents theoretical values, while the black line shows measured values in a plasma tube for nitrogen. In our study, the product Rp varies from approximately 500 cm·Pa to 1500 cm·Pa. Apply our values Rp to this range in Fig. 10, the reduced electric field (black line) remains constant despite variations in pressure and radius of the positive column, with a value of approximately 4 V/(cm·mmHg), which corresponds to $E/N \approx 1.3\times10^{-20}$ V·m^2.

To explain why the reduced electric field remains invariant despite changes in background gas number den-

sity, we consider that electron motion from cathode to anode is driven primarily by the electric field. Motion in other directions is negligibly small compared to drift motion and can be disregarded. The kinetic energy of an electron equals the energy gained from the electric field between consecutive collisions:

$$\frac{1}{2}m_e v_e^2 = eE\lambda \tag{12}$$

where m_e is the electron mass and λ is the mean free path. For sustaining glow discharge plasma, electrons must possess sufficient thermal energy for effective collisional ionization of gas molecules. Consequently, to maintain the discharge, the energy that an electron gains from the electric field between consecutive collisions must remain constant. Since the mean free path λ is inversely proportional to the gas number density N, the electric field E must be directly proportional to N, resulting in a constant reduced electric field E/N. Additionally, maintaining constant electron thermal energy ensures constant drift velocity, which further reinforces the requirement for a constant reduced electric field.

4.4. Electron density in positive column

According to Badaloni [21], the electron drift velocity can be calculated as:

$$v_e = 4.9 \times 10^{18} \left(\frac{E}{N}\right)^{0.7} \tag{13}$$

Applying this to Eq. (2), we determined the electron density across various pressure conditions, as presented in Fig. 11. The data shows a trend of increasing electron number density with increasing pressure, which agrees with results reported by Jassim [22].

In a positive column interacting with a shock wave in hypersonic flow, electron velocities significantly exceed the flow velocity. This allows us to neglect flow effects and conceptualize the shock wave as a boundary separating the positive column into two distinct segments operating in stationary air at different pressures. Our results demonstrate that the reduced electric field remains constant despite pressure variations. Consequently, when an oblique shock wave interacts with the positive column, as shown in Fig. 12, the reduced electric field appears to be equal upstream and downstream of the shock wave. This finding contradicts previous probe measurements, which reported a 3.75-fold increase in the reduced electric field downstream of the shock wave [23]. From visual analysis, we estimate that the column radius downstream of the shock wave decreases to approximately 0.7 of its upstream value. In a previous study [24], we assumed that the probe measurements of the reduced electric field gave correct values and, using Eq. (2) under constant current conditions, concluded that electron number density remains constant along the column even though the pressure and radius of column change across the shock wave.

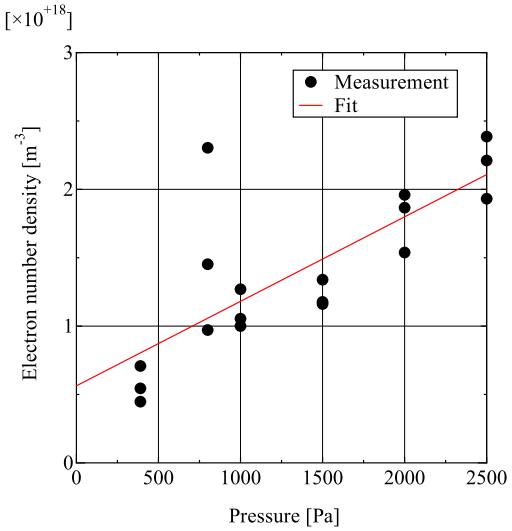

Fig. 11 Electron number density at various pressures

In the present study, the mean free path at 390 Pa corresponds to the uniform flow, and at 2000 Pa corresponds to conditions behind the shock wave in the aforementioned probe measurement study. From Fig. 8, we observe that the radius ratio between 2000 Pa and 390 Pa closely matches the radius ratio between the downstream and upstream regions of the shock wave in the probe measurements. This demonstrates that the positive column in hypersonic flow can be successfully simulated by that in stationary air conditions. However, our current investigation shows that electron density increases with pressure, which contradicts the conclusion mentioned in the previous paragraph. Therefore, a re-examination of the probe measurements is necessary.

As evident in Fig. 12, significant emission occurs at

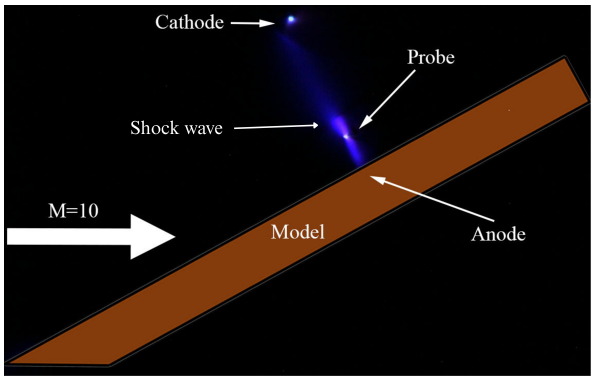

Fig. 12 Visualization of positive column with a probe inserted behind the shock wave

the probe tip. Experimental observations indicate that localized and strong emission occurs stochastically and is more common in hypersonic flows and in stationary air at high pressures. The phenomenon that induced this localized emission can substantially elevate the measured potential compared to an inherent floating potential. We propose that this probe-induced phenomenon is likely responsible for the artificially elevated potential and consequently the erroneously high calculated reduced electric field values behind the shock wave.

5. Conclusions

In this study, we investigated the emission intensity characteristics of positive columns in stationary air with mean free paths comparable to those in our hypersonic flow facility. Our analysis reveals that the emission intensity depends not only on the electron mean free path but also on the current density. These findings advance our understanding of flow visualization methods using glow discharge and offer a basis for quantitative flow measurements. Furthermore, this research contributes valuable insights into glow discharge behavior in low-pressure air without plasma tubes. Our results demonstrate systematic trends in several discharge parameters as pressure increases: electron number density increases, electrode gap voltage rises, and the radius of the positive column decreases. Despite these variations, the reduced electric field remains remarkably constant at approximately 1.3×10^{-20} V·m^2 across our experimental pressure range.

References

(1) Hanson, R., “Laser-Based Diagnostics for Hypersonic Flows,” *New Trends in Instrumentation for Hypersonic Research*, Springer, 1993, pp. 185–194.

(2) Exton, R., “Absorption, Scattering, and Fluorescence Techniques for Hypersonic Flow Measurements,” *New Trends in Instrumentation for Hypersonic Research*, Springer, 1993, pp. 205–214.

(3) Meier, U., Plath, I., and Kohse-Höinghaus, K., “Determination of Minority Species Concentrations and Temperature in Combustion Systems by Laser-Induced Fluorescence,” *New Trends in Instrumentation for Hypersonic Research*, Springer, 1993, pp. 195–204.

(4) Muntz, E. and Erwin, D., “Rapid Pulse Electron Beam Fluorescence for Flow Field Diagnostics,” *New Trends in Instrumentation for Hypersonic Research*, Springer, 1993, pp. 265–273.

(5) Nishio, M. and Itoh, H., “Second Electric Discharge Method for Visualizing Three-Dimensional Shock Shapes around Hypersonic Vehicles,” *Transactions of the Japan Society for Aeronautical and Space Sciences*, Vol. 38, No. 119, 1995, pp. 38–45.

(6) McCroskey, W., Bogdonoff, S., and McDougall, J., “An Experimental Model for the Sharp Flat Plate in Rarefied Hvnersonic Flow,” *AIAA Journal*, Vol. 4, No. 9, 1966, pp. 1580–1587.

(7) Horstman, C. and Kussoy, M. I., “Hypersonic Viscous Interaction on Slender Cones.” *AIAA Journal*, Vol. 6, No. 12, 1968, pp. 2364–2371.

(8) Fisher, S. and Bharathan, D., “Glow-Discharge Flow Visualization in Low-Density Free Jets,” *Journal of Spacecraft and Rockets*, Vol. 10, No. 10, 1973, pp. 658–662.

(9) Kimura, T., Nishio, M., Fujita, T., and Maeno, R., “Visualization of Shock Wave by Electric Discharge,” *AIAA Journal*, Vol. 15, No. 5, 1977, pp. 611–612.

(10) Jiang, W., Qiu, H., Yang, Y., Shi, Y., Wang, J., Li, J., Long, Z., and Mao, C., “High Frequency AC Electric Glow Discharge Visualization Technol-

ogy and Application in Big Diameter Hypersonic Low-Density Wind Tunnel," *Advances in Aerodynamics*, Vol. 3, No. 14, 2021.

(11) Itoh, H., "Glow Discharge-Tracer Technique for Velocity Profile Measurement in Hypersonic Boundary Layer Flows," *Journal of the Japan Society for Aeronautical and Space Sciences*, Vol. 53, No. 615, 2005, pp. 154–159 (in Japanese).

(12) Kimmel, R., Adamczak, D., Gaitonde, D., Rougeux, A., and Hayes, J., "HIFiRE-1 Boundary Layer Transition Experiment Design," *45th AIAA Aerospace Sciences Meeting and Exhibit*, 2007, p. 534.

(13) Nishio, M. and Itoh, H., "A Qualitative Theory for Visualizing Three Dimensional Shock Waves around Hypersonic Vehicles Using Electric Discharge," *Transactions of the Japan Society for Aeronautical and Space Sciences*, Vol. 37, No. 117, 1994, pp. 208–216.

(14) Itoh, H. and Mizoguchi, M., "Potential of Glow-Discharge Flow Measurement in Hypersonic Low-Density Flows," *AIAA Journal*, Vol. 58, No. 1, 2020, pp. 291–303.

(15) Rybkin, V., Titov, V., Kuvaldina, E., and Smirnov, S., "Concentration of Atomic Oxygen in the Positive Column of an Air Glow Discharge," *High Energy Chemistry*, Vol. 31, No. 2, 1997, pp. 128–131.

(16) Brown, S. C. and Singer, S., *Basic Data of Plasma Physics*, The Technology Press of the Massachusetts Institute of Technology, Cambridge; Wiley, New York; and Chapman and Hall, London, 1959, pp. 47–98.

(17) Itoh, H. and Mizoguchi, M., "On the Characteristics of an Electric Discharge Generated Across a Shock Wave in a Hypersonic Flow," *Journal of the Japan Society for Aeronautical and Space Sciences*, Vol. 51, No. 599, 2003, pp. 653–658 (in Japanese).

(18) ARTRAY CO., LTD., "USB2.0 Ultraviolet CCD Camera ARTCAM-407UV-WOM Series Instruction Booklet Ver1.05," 2023.

(19) Baryshnikov, A. S., Basargin, I., Bobashev, S. V., Monakhov, N. A., Popov, P., Sakharov, V., and Chistyakova, M. V., "Interaction of Shock Wave with Free Glow Discharge," *Technical Physics Letters*, Vol. 43, 2017, pp. 511–513.

(20) Raizer, Y. P. and Allen, J. E., *Gas Discharge Physics*, Vol. 1, Springer, 1991.

(21) Badaloni, S., "Basic data of air discharges," *Rep. of Padova Univ.*, 1972.

(22) Jassim, M. K., "Investigation in the Effect of Applied Voltage and Working Pressure on Some Plasma Parameters in the Positive Column of Dc Glow Discharge," *Ibn AL-Haitham Journal For Pure and Applied Sciences*, Vol. 32, No. 2, 2019, pp. 9–20.

(23) Uenaka, A., "Probing of Discharged Plasma Generated for Hypersonic Flow Measurement," Master's Thesis, National Defense Academy of Japan, 2023 (in Japanese).

(24) Van, N. C., Itoh, H., Mizoguchi, M., and Uenaka, A., "Electric Field Measurement in Glow Discharge Plasma Interacting with Shock Wave in Hypersonic Flow," *34th Congress of the International Council of the Aeronautical Sciences*, No. 7.6.4, 2024.